DNA Damage, RAD9 and Fertility/ Infertility of *Echinococcus granulosus* Hydatid Cysts

GONZALO CABRERA,[1] MARÍA EUGENIA CABREJOS,[2] ALESSANDRA LOUREIRO MORASSUTTI,[3] CAROLINA CABEZÓN,[1] JUANA ORELLANA,[4] ULF HELLMAN,[5] ARNALDO ZAHA,[3] AND NORBEL GALANTI[1]*

[1] *Programa Disciplinario de Biología Celular y Molecular, Instituto de Ciencias Biomédicas, Facultad de Medicina, Universidad de Chile, Santiago, Chile*

[2] *Aquainnovo S.A., Puerto Montt, Chile*

[3] *Laboratório de Biologia Molecular de Cestódeos, Centro de Biotecnologia, Universidade Federal do Rio Grande do Sul, Porto Alegre, RS, Brazil*

[4] *Programa Disciplinario de Inmunología, Instituto de Ciencias Biomédicas, Facultad de Medicina, Universidad de Chile, Santiago, Chile*

[5] *Laboratory of Protein Structure, Ludwig Institute for Cancer Research, Uppsala, Sweden*

Hydatidosis, caused by the larval stage of the platyhelminth parasite *Echinococcus granulosus*, affects human and animal health. Hydatid fertile cysts are formed in intermediate hosts (human and herbivores) producing protoscoleces, the infective form to canines, at their germinal layers. Infertile cysts are also formed, but they are unable to produce protoscoleces. The molecular mechanisms involved in hydatid cysts fertility/infertility are unknown. Nevertheless, previous work from our laboratory has suggested that apoptosis is involved in hydatid cyst infertility and death. On the other hand, fertile hydatid cysts can resist oxidative damage due to reactive oxygen and nitrogen species. On these foundations, we have postulated that when oxidative damage of DNA in the germinal layers exceeds the capability of DNA repair mechanisms, apoptosis is triggered and hydatid cysts infertility occurs. We describe a much higher percentage of nuclei with oxidative DNA damage in dead protoscoleces and in the germinal layer of infertile cysts than in fertile cysts, suggesting that DNA repair mechanisms are active in fertile cysts. rad9, a conserved gene, plays a key role in cell cycle checkpoint modulation and DNA repair. We found that RAD9 of *E. granulosus* (EgRAD9) is expressed at the mRNA and protein levels. As it was found in other eukaryotes, EgRAD9 is hyperphosphorylated in response to DNA damage. Our results suggest that molecules involved in DNA repair in the germinal layer of fertile hydatid cysts and in protoscoleces, such as EgRAD9, may allow preserving the fertility of hydatid cysts in the presence of ROS and RNS.

Hydatidosis is a cosmopolitan zoonosis caused by the larval (metacestode) stage of the tapeworm *Echinococcus granulosus* and represents a major public health and economic burden in many countries (Eckert and Deplazes, 2004; Budke, 2006).

The metacestode develops in internal organs (mainly liver and lungs) of humans and other intermediate hosts as unilocular fluid-filled bladders (McManus et al., 2003). The hydatid cyst is composed of three layers: an inner cellular germinal layer (GL) that is supported externally by a tough elastic non-cellular laminated layer (LL), which in turn is surrounded by a host-produced adventitial layer (Bortoletti and Ferretti, 1978; Martinez et al., 2005). Protoscoleces (PSc), the developmental forms of the parasite, infective to definitive host (canines), emerge from the GL of fertile hydatid cysts. Infertile hydatid cysts do not produce PSc (Bortoletti and Ferretti, 1978; Kamenetzky et al., 2000).

In *E. granulosus* infections, Th1 cell activation, characterized by an increase in interleukin (IL)-2, interferon-gamma (IFN-γ), and tumoral necrosis factor (TNF)-α is related to protective immunity to the host. On the other hand, Th2 cell activation, involving elevated IL-4, IL-5 and IL-10 is related to susceptibility to the disease (Shepherd et al., 1991; Rigano et al., 1995; Rigano et al., 2007). The mechanism by which a Th1-type response determines the protection of the host remains unclear. Nevertheless, it can be hypothesized that Th1 cytokines would promote cell recruitment, mostly macrophages, around the hydatid cyst, and their activation induce the production of free radicals, such as superoxide anion by NADPH oxidase and nitric oxide by inducible nitric oxide synthase (iNOS) (Dzik, 2006). These free radicals have well documented antiparasitic activity

Abbreviations: 8-oxo-dG, 8-Oxo-7,8-dihydro-2′-deoxyguanosine; *E. granulosus*, *Echinococcus granulosus*; EgRAD9, *Echinococcus granulosus* RAD9; EgEF1, *Echinococcus granulosus* EF1; PSc, protoscoleces; GL, germinal layer; FGL, fertile germinal layer; IGL, infertile germinal layer; ROS, reactive oxygen species; RNS, reactive nitrogen species; CIP, calf intestinal alkaline phosphatase.

Contract grant sponsor: FONDECYT-Chile;
Contract grant numbers: 1010817, 1050135.
Contract grant sponsor: RTPD/Network.
Contract grant sponsor: SIDA/SAREC.

*Correspondence to: Norbel Galanti, Programa Disciplinario de Biología Celular y Molecular, Instituto de Ciencias Biomédicas, Facultad de Medicina, Universidad de Chile, Independencia 1027, Casilla 70061, Correo 7, Santiago, Chile.
E-mail: ngalanti@med.uchile.cl

in *Leishmania* (Hirji et al., 1998) and *Schistosoma* (James and Glaven, 1989). Thus, in humans, elevated levels of nitric oxide and IFN-γ have been observed in sera from patients with *E. granulosus* infections (Touil-Boukoffa et al., 1998). Moreover, exposure of hydatid cysts to an experimental source of nitric oxide (S-nitroso-N-acetylpenicillamine) or to IFN-γ activated macrophages resulted in significant cyst damage, suggesting an antihydatid activity by ROS and RNS (Steers et al., 2001). Nevertheless, this effect was observed only after 3 days of incubation, suggesting the presence of molecular protection against these reactive species.

Even though most cellular macromolecules may be targeted by free radicals species, primary alterations due to oxidative stress usually derive from DNA damage (Riley, 1994; Wang et al., 1998). The outcome of DNA damage is diverse and generally adverse. Acute effects arise from disturbed DNA metabolism, triggering cell-cycle arrest or cell death (Hoeijmakers, 2001). In order to maintain genomic stability, eukaryotic cells utilize a network of checkpoint and DNA repair proteins upon DNA damage (Zhou and Elledge, 2000). Studies in yeast and human have shown that the evolutionarily conserved protein RAD9 plays key roles both in checkpoint activation and in DNA repair (Parrilla-Castellar et al., 2004; Lieberman, 2006). In response to genotoxic damage, RAD9 can form a heterotrimer with RAD1 and HUS1 (9-1-1 complex) which resembles a proliferating cell nuclear antigen (PCNA)-like sliding clamp (Thelen et al., 1999; Venclovas and Thelen, 2000). As a part of this protein complex, RAD9 acts as a DNA damage sensor and is loaded around DNA (Volkmer and Karnitz, 1999; Roos-Mattjus et al., 2002). The DNA-bound 9-1-1 complex then facilitates ATR-mediated phosphorylation and activation of Chk1 (Roos-Mattjus et al., 2003), a protein kinase that regulates S-phase progression (Kaneko et al., 1999) and G2/M arrest (Liu et al., 2000). In addition to its role in checkpoint activation, RAD9 may participate directly in DNA repair since the protein (along with RAD1 and HUS1) presents the ability to bind the DNA glycosylase MYH (Chang and Lu, 2005). Also RAD9 stimulates the activation of the apurinic/apyrimidinic endonuclease 1 and DNA polymerase beta, in long patch base excision repair (Gembka et al., 2007). Recently, it was found that *Schizosaccharomyces pombe* overexpressing the *rad9* gene showed higher survival in minimal media containing sodium nitroprusside as a source of nitric oxide (Kang et al., 2007).

The present work was designed to determine the participation of oxidative DNA damage in triggering the infertility of hydatid cysts and the death of PSc. In agreement with this proposal, we found a much higher percentage of nuclei with DNA damage in the germinal layer of infertile cysts and in death protoscoleces, when compared to fertile cysts. In addition, we characterized the *rad9* gene of *E. granulosus* (*Egrad9*) as well as its expression at the mRNA and protein levels (genebank accession EU276122). Finally, we found that RAD9 is hyperphosphorylated in response to ROS aggression.

Materials and Methods

Hydatid cysts and protoscoleces

Fresh, fertile and infertile *E. granulosus* hydatid cysts were obtained from bovine (*Bos taurus*) livers or lungs at abattoirs in Santiago, Chile and processed as previously described (Galindo et al., 2003; Martinez et al., 2005). Macroscopically, a cyst is fertile when it presents free Psc in the hydatid fluid, whitish color of the germinal and laminar layers and a thick laminar layer (Bortoletti and Ferretti, 1978). Fertility was confirmed by presence of protoscoleces in the hydatid fluid (Galindo et al., 2003). Germinal layer from fertile (FGL) and infertile (IGL) cysts as well as PSc, were obtained as indicated (Paredes et al., 2007). Psc were decanted by gravity from the hydatid fluid, and treated as described (Galindo et al., 2002).

DNA damage determination and localization in hydatid cyst germinal layers and in protoscoleces

Immunodetection of 8-oxo-dG adducts was performed as previously described (Machella et al., 2005) with some modifications. Pieces of GLs from fertile and infertile hydatid cysts and pepsinated PSc, were fixed in 4% paraformaldehyde for 24 h at 4°C. After dehydration, samples were embedded in Paraplast® and 5 μm sections were placed on xylanized slides. Sections were incubated at 37°C for 1 h with 100 μg/ml RNase in Tris buffer (10 mM Trizma base, 1 mM EDTA, 0.4 M NaCl, at pH 7.5) and washed twice in PBS. Proteins were removed from DNA by digestion with proteinase K (10 μg/ml in Tris buffer at pH 7.5) at room temperature for 10 min. To increase the antibody accessibility to the antigen, a denaturation step with 2 N HCl for 10 min was applied, followed by neutralization with Tris buffer for 5 min. Slides were blocked overnight with Cas-Block (Zymed, San Francisco, CA) and incubated with monoclonal mouse antibodies anti 8-oxo-dG (Chemicon International, Temecula, CA) 1:50 v/v, followed by polyclonal fluoride conjugated anti mouse IgG (Molecular Probes Inc., Eugene, OR) 1:300 v/v. Afterwards, slides were mounted in Vectashield® and visualized in a Nikon Eclipse E400 epifluorescence microscope. The percentage of nuclei presenting DNA damage was obtained by scoring 8-oxo-dG positive reaction in 500 nuclei. The statistical significance of differences between FGLs and IGLs were calculated by the Student's *t*-test. As a control for the technique, PSc were treated with 1 or 10 mM H_2O_2 for 1 h at 37°C, before the determination of 8-oxo-dG.

Sequencing and molecular characterization of Egrad9

E. granulosus EST clones homologous to human Rad9 (hRad9) protein were searched using the TBLASTX program (http://www.ncbi.nlm.nih.gov/blast) in the *E. granulosus* freely available database (http://www.nematodes.org/neglectedgenomes/lopho/lophdb.php) (Fernández and Maizels, personal communication). The *Egrad9* clones were kindly provided by Dr. Cecilia Fernandez. The identity of these clones was confirmed by DNA sequencing. The alignments were performed using Clustal W and T-Coffee programs. Modeling of EgRAD9 tertiary structure was obtained from the derived primary amino acid sequence using the Phyre (Protein homology/analog recognition gene) program version 0.2 (http://www.sbg.bio.ic.ac.uk/~phyre/).

Egrad9 mRNA expression in prostoscoleces and in germinal layers from fertile and infertile hydatid cysts

Total RNA was extracted from freshly isolated PSc, FGL, and IGL with Trizol reagent (Gibco BLR, Grand Island, NY) and isolated following the manufacturer's instructions. The RNA obtained was treated with RQ1 RNase-Free DNase (Promega, Madison, WI), and the corresponding cDNAs were obtained, using the Thermoscript RT-PCR System (Invitrogen, Carlsbad, CA). For identification of *Egrad9* mRNA expression, specific *E. granulosus* oligonucleotides were designed (forward 5′-AAGGTTTTTACCA-GGGCTATTTC-3′ and reverse 5′-GACCAGTTTCTAGGCGC-ATT-3′, with an expected size of 277 bp). For the identification of a common housekeeping β-actin gene from *E. granulosus* (Genebank accession No. 3831419, da Silva et al., 1993) and *B. taurus* (Genebank accession No. 27819613, Davey et al., 1995) we designed oligonucleotides with 100% identity, using the Clustal W 1.83 program (5′-GACATGGAGAAGATCTGGC-3′ and 5′-GCCATTTCGTTCTCAAAGTC-3′). The expected length of this fragment is 443 bp in both species. The RT-PCR reactions were carried out in a 12.5 μl volume, containing 1 μl of cDNA, 3 mM of $MgCl_2$, 0.2 mM of each dNTP, 1.5 units of Taq polymerase (Invitrogen) and 16 pmol of each primer. The program used comprised 5 min of denaturation at 95°C, 38 cycles of 1 min at 95°C, 1 min at 59°C, and 1 min at 72°C, followed by a final extension reaction of 7 min at 72°C.

Egrad9 mRNA localization in prostoscoleces

A DNA sequence spanning nt 92–368 (277 bp) of *Egrad9* cDNA was cloned in the pGEM-T-easy vector (Promega) and an antisense digoxigenin-labeled riboprobe was generated. Histological processing and probe hybridization were performed as previously described (Gutfeld et al., 2006).

Preparation and purification EgRAD9 and EgEF1 polyclonal antibodies

The Egrad9 cDNA region encoding the C-terminal fragment of EgRAD9 (amino acids 262–420), was amplified from total cDNA by PCR using Platinum Taq High Fidelity polymerase (Invitrogen) and the primers forward (5′-ACGGGATCCTTACCGTACTTCCC-AACG-3′) with a *Bam* HI restriction fragment, and reverse (5′-GGCAAAGTGGGTCAAGTTCTCGAGTCA-3′), with a *Xho* I restriction fragment (enzyme that produces compatible end with *Sal I*). As a housekeeping protein, the *Egef1* cDNA region encoding the N-terminal fragment of EgEF1 (amino acids 16–126) was amplified from total cDNA as above, using the primers forward (5′-CACGGATCCCCAAATTATCACGAGATGGAG-3′) with a *Bam* HI restriction fragment and reverse (5′-CAATGTCGACGTCAT-CACCGCCTTCAGC-3′), with a *Sal* I restriction fragment. Both restriction digestion created cohesive ends for oriented ligation into the plasmid expression vector pQE-80L (Qiagen Inc., Valencia, CA). The resulting fusion proteins carried N-terminal His-Tag sequence. Recombinant plasmids were transformed into competent *Escherichia coli* BL21 (DE3) pLys S. Synthesis of recombinant EgRAD9-His and EgEF1-His proteins were induced with 1 mM IPTG (isopropylthio-β-galactoside) overnight at 37°C. The identity of these proteins was confirmed by Maldi-ToF. The fusion proteins were purified under denaturant conditions, using Ni-NTA (Invitrogen) resin and following the manufacturer's recommendations. These proteins were used to prepare rabbit antiserum. The titer was checked 1 week after each injection by ELISA. Finally, the specific polyclonal antibodies were purified as previously described (Rucklidge et al., 1996).

Identification of EgRAD9 and EgRAD9 phosphorylated forms by Western blot

Samples from FGL, IGL, PSc and control primary culture bovine lung cells were lysed in 1% SDS, 10 mM Tris, 5 μg/ml Aprotinin, 1 mM EDTA, 5 mM PMSF, 1 mM TPCK. *Western blots* of total proteins (Bradford, 1976), separated in 10% SDS–polyacrylamide gels, were reacted with a rabbit polyclonal antibody anti recombinant fragment EgRAD9 or EgEF1, followed by secondary antibodies, conjugated to horseradish peroxidase (Jackson No. 111-035-144). To identify EgRAD9 phosphorylated forms, aliquots were treated with 20 U of calf intestinal alkaline phosphatase (CIP) (Promega) 30 min at 30°C, electrophoresed through 10% SDS–polyacrylamide gels, and immunoblotted with polyclonal antibody anti EgRAD9, essentially as above.

Results

Oxidative DNA damage in protoscoleces exposed to different concentrations of hydrogen peroxide

Detection of 8-oxo-dG, a typical DNA modification generated by ROS and RNS (Fraga et al., 1990), was performed in histological sections of FGL, IGL, and PSc, using a monoclonal anti-8-oxo-dG antibody. Results for control PSc, non-treated with H_2O_2 and PSc treated with 1 mM or 10 mM H_2O_2 for 1 h at 37°C, are shown in Figure 1A–C, respectively. A gradual increase in the number of positive nuclei for 8-oxo-dG (in green), indicative of oxidative DNA damage resulting from treatment with increased levels of hydrogen peroxide, was observed. Fluorescence was not detected in histological sections of PSc treated with 10 mM H_2O_2 and incubated only with the secondary antibody (Fig. 1D), indicative of the specificity of the reaction. These results show that ROS generates oxidative damage in the DNA of *E. granulosus* PSc.

Figure 2 shows representative Hoechst, 8-oxo-dG and 8-oxo-dG/Hoechst merged images of the germinal layer from hydatid cysts and PSc. Generally, no positive 8-oxo-dG reaction was observed in nuclei from fertile cysts. However, in a few

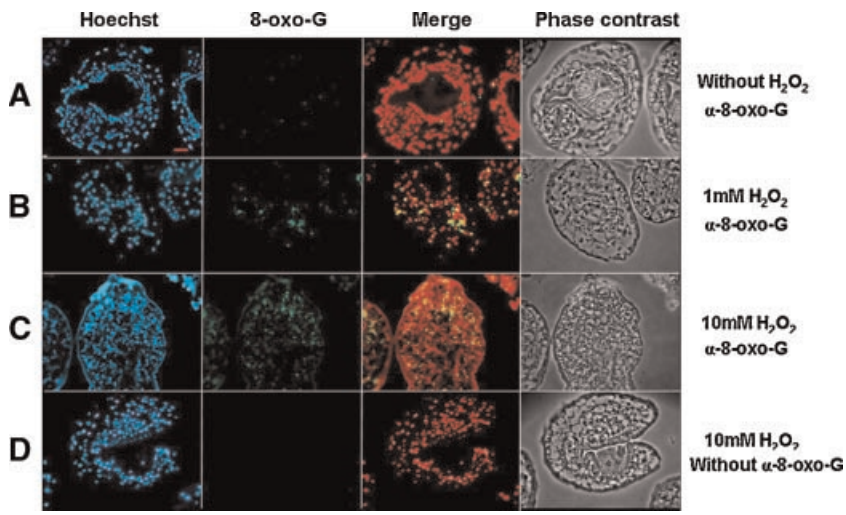

Fig. 1. Oxidative DNA damage in protoscoleces exposed to different concentrations of hydrogen peroxide in vitro, as determined by 8-oxo-dG immunolocalization. PSc non-treated (A) or treated with 1 mM H_2O_2 (B) or 10 mM H_2O_2 (C,D) were incubated with anti-8-oxo-dG mouse primary monoclonal antibody (Chemicon) (A–C). The immune complexes were detected using a secondary anti-mouse antibody conjugated to Alexa 488 (A–D). Hoechst was used for nuclear staining. Parts (B,C) show positive 8-oxo-dG nuclei (green). Merge 8-oxo-dG/Hoechst in pseudo color red; yellow corresponds to colocalization of both colors. Bar: 10 μm. [Color figure can be viewed in the online issue, which is available at www.interscience.wiley.com.]

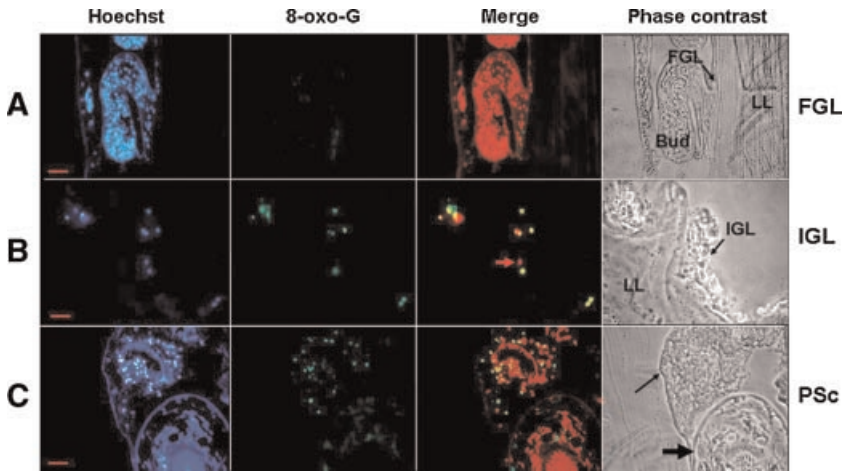

Fig. 2. Oxidative DNA damage in fertile and infertile hydatid cysts and in PSc in vivo, as determined by 8-oxo-dG immunolocalization. Histological sections of the germinal layer from fertile cysts (A), infertile cysts (B) and PSc (C). Nuclear staining and 8-oxo-dG detection were as indicated under Figure 1. Positive 8-oxo-dG nuclei merged with red Hoechst in pseudo color (yellow) corresponds to colocalization of both dyes. Bars: 10 μm. GL, germinal layer; LL, laminated layer; thick arrow, viable protoscolex; thin arrow, degenerated protoscolex. Percentage of nuclei with oxidative DNA damage: FGL: 14.77 ± 2.97%, n = 3 and IGL: 64.45 ± 7.15%, n = 2. FGL, fertile germinal layer; IGL, infertile germinal layer. [Color figure can be viewed in the online issue, which is available at www.interscience.wiley.com.]

areas of the germinal layer, mainly those not related with PSc formation, it is possible to find some nuclei showing DNA damage (data not shown). Contrarily, the germinal layer of infertile cysts presents nuclei clearly showing DNA damage (Fig. 2B), though it is still possible to find some nuclei without DNA damage (Fig. 2B, arrow). PSc presenting loss of tegument continuity (Fig. 2C, thin arrow) show higher levels of oxidative DNA damage than PSc with intact tegument (Fig. 2C, thick arrows). Importantly, DNA damage showed in Figure 2 corresponds to in vivo occurrences in the germinal layer and in PSc of hydatid cysts, as these have not been treated with peroxide or other oxidative agent. The percentage of nuclei showing oxidative DNA damage in the germinal layer of infertile hydatid cysts was significantly higher (64.45 ± 7.15%) than the one observed in the germinal layer of fertile cysts (14.77 ± 2.97%).

These results clearly suggest that oxidative damage of DNA is part of an infertility-inducing mechanism in *E. granulosus* hydatid cysts and in the death of PSc.

Identification and characterization of Egrad9 gene

An expressed sequence tag (EST), bearing significant homology to human Rad9 (hRad9) gene, was detected from the cDNA database of *E. granulosus* using the TBLASTX program. We isolated and sequenced the entire nucleotide *Egrad9* cDNA (1,365 pb, Genebank accession No. EU276122). A 61 bp 5′ untranslated region, a 1,272 bp open reading frame and a 32 pb 3′ untranslated region are present. The deduced amino acid sequence (Genebank accession No. ABX71160) codes for 423 amino acid residues with a predicted molecular mass and isoelectric point of 46 kDa and 5.24, respectively (Fig. 3A). A domain (amino acids 1–331) typical of the RAD9 family is present in our deduced EgRAD9 sequence. Using the Phyre (Protein Homology/Analog Recognition Gene) program version 0.2, we generated a model for EgRAD9 tertiary structure (based on human PCNA crystallographic structure) with high similarity to DDC1 (RAD9) structures from *Saccharomyces cerevisiae* (Fig. 3B) (Venclovas and Thelen, 2000).

Figure 3C shows the alignment of the deduced amino acid sequence EgRAD9 with other eukaryotic RAD9 sequences. EgRAD9 shared 25% of amino acid identity with Rad9 from *Homo sapiens* (Genbank accession No. NP_004575), 22% from *B. taurus* (Genbank accession No. AAX08663), 19% from *S. pombe* (Genbank accession No. CAA54491), 18% from *Drosophila melanogaster* (Genbank accession No. AAL28664) and 15% to HPR9 (RAD9) from *Caenorhabditis elegans* (Genbank accession No. NP_499342). Interestingly, phylogenetic analysis showed that the EgRAD9 protein is closer to vertebrates than nematodes, yeast and *Drosophila* (Fig. 3C). This result is not unexpected considering the present location of platyhelminthes in the evolutionary tree (Adoutte et al., 2000).

mRNA expression of Egrad9 in the germinal layer of hydatid cysts and protoscoleces

The mRNA expression of *Egrad9* in the germinal layer of fertile and infertile cysts as well as in PSc was assessed by RT-PCR analysis (Fig. 4A). We detected *Egrad9* transcripts in PSc (lane 2), FGL (lane 3) and in IGL (lane 4). *Egrad9* was not detected in bovine hepatic tissue cDNA (lane 5). As a control of cDNA synthesis we used common *E. granulosus* and *B. taurus* housekeeping β-actin gene oligonucleotides. We detected the β-actin genes in all the samples (Fig. 4B).

Egrad9 mRNA localization in prostoscoleces

As observed in Figure 4C, the *Egrad9* antisense digoxigenin-labeled riboprobe generated from nucleotides 92 to 368 (277 bp) is distributed throughout the entire PSc structures, mainly in zones with a greater nuclear density.

EgRAD9 identification by Western blot

Using polyclonal antibodies anti-EgRAD9, the EgRAD9 protein was identified by *Western blot*, as a ~49 kDa protein in 1 mM H_2O_2 treated and non-treated PSc (Fig. 5A, lanes 1 and 2) as well as in FGL homogenates (Fig. 5A, lane 4). However, EgRAD9 was recognized as a ~52 kDa in 10 mM H_2O_2 treated PSc homogenates (Fig. 5A, lane 3). Densitometric analysis of the bands corresponding to EgRAD9 was normalized to the housekeeping EgEF1 protein. Levels of expression of EgRAD9 were similar in the different samples analyzed. The EgRAD9

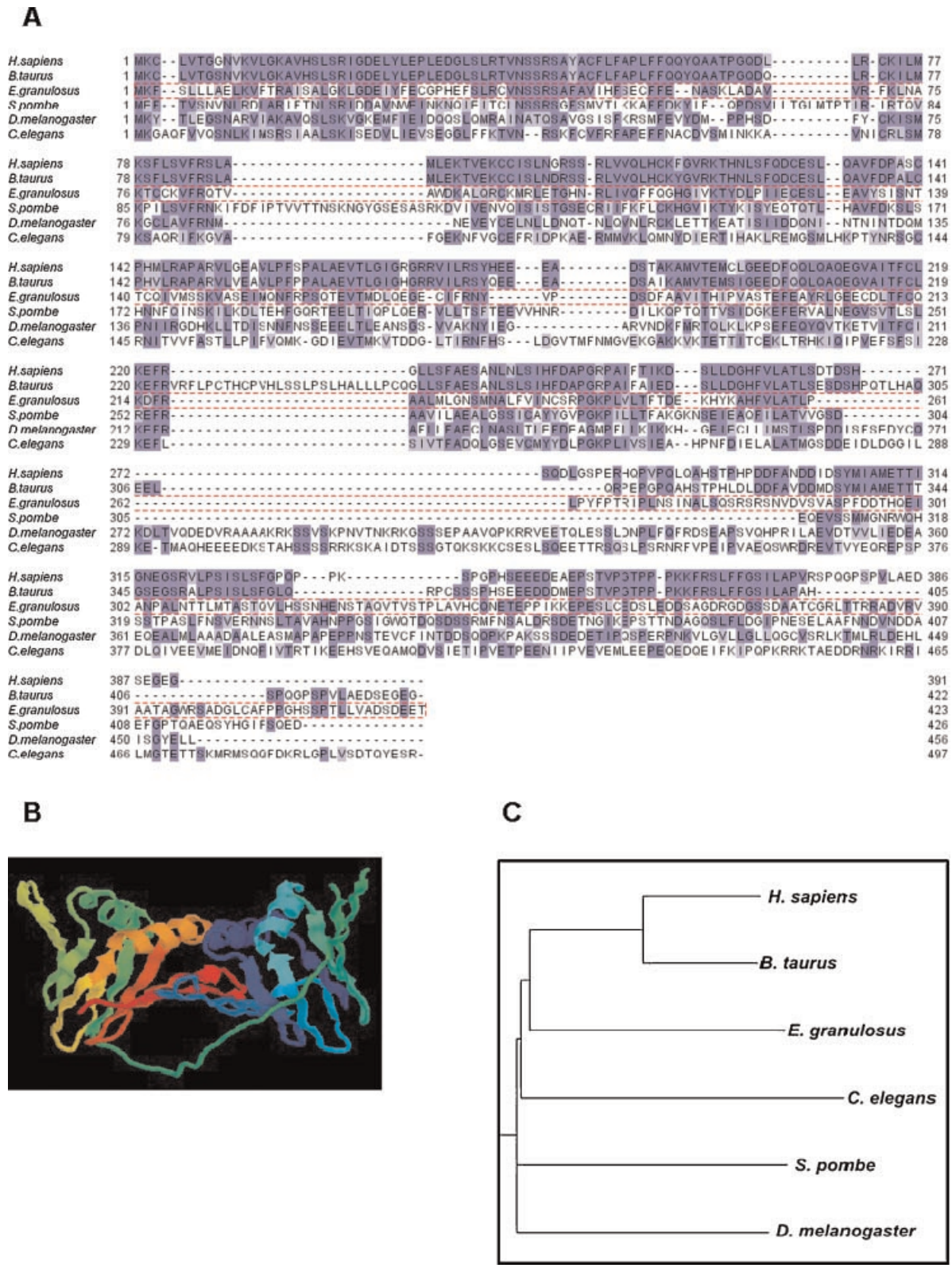

Fig. 3. *E. granulosus* rad9 (*Egrad9*) gene. A: *Egrad9* cDNA sequence. The initial (ATG) and stop (TGA) codons are underlined. Coding sequences are shown in dark gray bold letters; 3′ and 5′ UTR regions sequences in light gray. B: EgRAD9 predicted translation product. Rad9 family domain is shown between arrows (residues 1–331). C: Model of EgRAD9 tertiary structure obtained from the predicted translation product using Phyre, Protein homology/analog recognition gene, program version 0.2. [Color figure can be viewed in the online issue, which is available at www.interscience.wiley.com.]

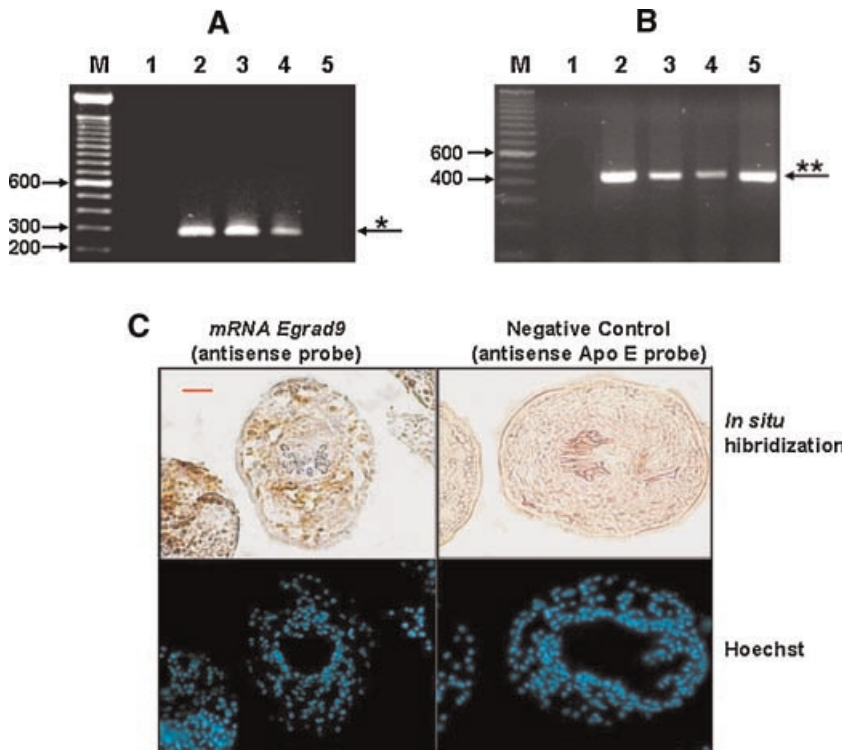

Fig. 4. ***Egrad9*** **mRNA expression in hydatid cysts germinal layers and in protoscoleces. RT-PCR amplification of** ***Egrad9**** **(A) and** ***β-actin***** **(B) using total mRNA isolated from germinal layers of fertile and infertile hydatid cysts as well as PSc. Lane 1: negative control without DNA. Lanes 2, 3, 4 and 5 cDNA from PSc, bovine FGL, bovine IGL and bovine hepatic tissue, respectively. M: DNA Ladder 100 pb. C: PSc hybridized with digoxigenin-labeled anti-sense RNA probe directed against** ***Egrad9*** **or with anti-sense RNA probe directed against** ***ApoE*** **gene from zebra fish as a negative control. The reaction was developed using an alkaline phosphatase-conjugated anti-digoxigenin antibody. For nuclear staining Hoechst was used. Bar: 10 μm. [Color figure can be viewed in the online issue, which is available at www.interscience.wiley.com.]**

slower migrating band found in 10 mM H_2O_2 treated PSc could be a hyperphosphorylated form of the protein in response to DNA damage, as mentioned for hRad9 (St Onge et al., 1999; Volkmer and Karnitz, 1999; Yoshida et al., 2003). Analysis of EgRAD9 from IGL, though gave positive results, was not incorporated in the figure considering that this parasite structure is very thin and could carry bovine contamination.

Determination of EgRAD9 phosphorylated forms

Total protein extracts from PSc non-treated and treated with 10 mM H_2O_2 were either incubated or not with calf intestinal alkaline phosphatase (CIP). Samples were then subjected to *Western blot* analysis using anti-EgRAD9 antibody (Fig. 5B). After treatment with CIP only a ~46 kDa band is observed; this is the expected molecular weight for the non-phosphorylated form of RAD9. Similarly, treatment of FGL extracts with CIP produced the same decrease in the molecular mass of EgRAD9 (from ~49 to ~46 kDa, Fig. 5C). These results suggest that EgRAD9, as hRad9 (St Onge et al., 2003; Yoshida et al., 2003), is expressed constitutively as a ~49 kDa phosphorylated form and is hyperphosphorylated in response to DNA damage to a ~52 kDa form.

Discussion

Considering the structure of hydatid cysts, cells of the innate immune system, which are lodged in the adventitial layer, are unable to penetrate up to the germinal layer due to the physical barrier imposed by the laminar layer. We propose that the presence of the innate immune system cells at the adventitial layer, mainly macrophages, could be associated to the release of ROS and RNS (Werling et al., 2006), a mechanism through which the Th1-type response could provoke infertility and death of the hydatid cysts (Shepherd et al., 1991; Rigano et al., 1995, 2007; Vuitton, 2003). Our proposal is supported by in vitro observations that fully formed hydatid cysts are susceptible to the products of activated macrophages and in particular nitric oxide (Steers et al., 2001). Furthermore, in vivo studies have indicated the presence of nitric oxide and lipid peroxidation in the germinal layer and hydatid fluid of fertile and infertile cysts and PSc (Amanvermez and Celik, 2002). Most probably, the penetration of reactive species into the germinal layer of cysts would be through a chain reaction of the free radicals released by cells of the innate immune system lodged in the adventitial layer and non-radical molecules present in the laminar and germinal layers, generating a wave of reactive species (Webster and Nunn, 1988; Harman, 1992). We cannot discard an increase in the production of ROS and RNS by the same anabolic activity directly in the germinal layer.

The most frequently observed alteration of oxidative damage of DNA is the formation of 8-oxo-dG (Fraga et al., 1990). Indeed, we detected a higher number of nuclei positive to 8-oxo-dG in PSc treated with H_2O_2 in comparison with non-treated PSc. Moreover, PSc that are still associated to the FGL but in process of degeneration (those presenting a significant disorganization of morphological structures such as tegument and hooks), display higher levels of oxidative DNA damage when compared to PSc still retaining intact morphological

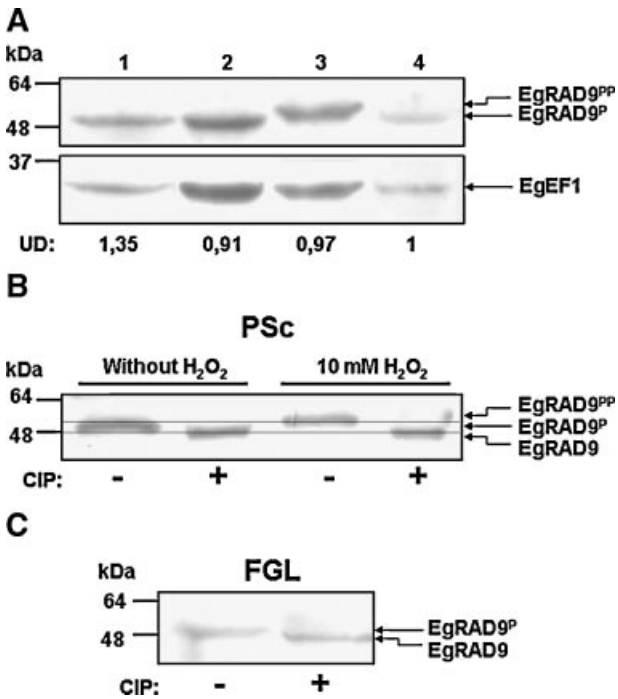

Fig. 5. Identification of EgRAD9 and its phosphorylated forms in hydatid cyst fertile germinal layer and in protoscoleces. A: Western-blot detection of EgRAD9. Total proteins extracted from FGL and PSc, treated and non-treated with hydrogen peroxide, were subjected to *Western blot* analysis using anti-EgRAD9 or anti-EgEF1 antibodies. Lane 1: Non-treated PSc. Lanes 2 and 3: PSc treated with 1 mM H_2O_2 or 10 mM H_2O_2, respectively. Lane 4: Bovine FGL. B: Phosphorylated forms of PSc EgRAD9 in response to hydrogen peroxide DNA damage. Total protein extracts from PSc treated or non-treated with 10 mM H_2O_2 were either incubated or not with CIP. Samples were then subjected to *Western blot* analysis using anti-EgRAD9 antibody. C: Phosphorylated forms of FGL EgRAD9 in vivo. Total protein extracts from FGL were incubated or not with CIP. Samples were then subjected to *Western blot* analysis using anti-EgRAD9 antibody.

characteristics (Fig. 2C). Similarly, we established that the percentage of nuclei with oxidative DNA damage in IGL is significantly higher than in FGL. Several studies show that in multicellular organisms, genotoxic products such as ROS and RNS may trigger apoptosis when DNA damage exceeds the possibilities of repair (Hoeijmakers, 2001). Accordingly, Paredes et al. (2007) have shown that PSc in degenerative processes display a high index of apoptotic nuclei and that IGL shows a higher apoptotic index when compared to FGL. These observations strongly suggest that oxidative DNA damage exceeds DNA repair mechanisms, triggering death of PSc and apoptosis in the germinal layer, leading to infertility of hydatid cysts. On the other hand, fertile hydatid cysts are able to generate changes in the pattern of cytokines in the host inducing a Th2-type response (Lopez-Moreno, 2002; Vuitton, 2003), probably diminishing the release of ROS and RNS by macrophages, ensuring the survival of the parasite.

It has been shown that *Echinococcus* is able to survive in aerobic environments, resisting the oxidative stress derived from ROS and RNS generated during the normal oxidative metabolism of the parasite (Conchedda et al., 2004) or as a result of the immune response of the host towards the infection (Callahan et al., 1988). Evidence showing that morphological alterations in FGL of *E. granulosus* appears only after 3 days of incubation with activated macrophages (Steers et al., 2001), suggest that mechanisms of DNA repair do exist. However, the molecules involved in cell-cycle arrest and/or repair of oxidative DNA damage in *E. granulosus* are unknown. Research in helminth organisms indicates the existence of base excision repair (BER) mechanisms in *Schistosoma mansoni* (Furtado et al., 2007), and the presence of HUS1, MRT2, and HPR9 proteins in *C elegans*, the last two orthologous to Rad1 and Rad9 in humans, respectively (Stergiou and Hengartner, 2004).

The *rad9* gene was isolated for the first time in *S. pombe* by Murray et al. (1991). Subsequently, explorations using *Southern blot* assay, or more frequently computer analyses using databases in cDNA libraries, revealed orthologous sequences of *rad9* of different species, such as *H. sapiens* (Lieberman et al., 1996), *D. melanogaster* (Dean et al., 1998) and *Gallus domesticus* (Kobayashi et al., 2004). The abilities of RAD9 to form the 9-1-1 heterotrimer (Volkmer and Karnitz, 1999), maintaining the protein tertiary structure (Venclovas and Thelen, 2000) and regulating cell progression, have been retained during the evolution, from yeast to human. Thus, ectopic expression of the human cognate, hRad9, in *S. pombe rad9* mutant can not only restore radioresistance but also complement the associated cell cycle checkpoint defects (Lieberman et al., 1996). In our hands, *rad9* gene in *E. granulosus* showed similar amino acid identity, tertiary structure and protein domains compared with RAD9 from other eukaryotic organisms suggesting evolutionary conservation of the functions. To our knowledge, this is the first DNA repair protein to be reported in *E. granulosus*.

A study using Northern blot analysis has established that mRNA of Rad9 from *Mus musculus* was expressed in all the tissues examined (Hang et al., 1998). Accordingly, we found that *Egrad9* messenger RNA is expressed in PSc, IGL, and FGL, and established the nuclear location of these transcripts in all cells of protoscoleces. It was demonstrated that cells with altered Rad9 expression are sensitive to DNA damage (Hang et al., 2000; Hopkins et al., 2004; Dang et al., 2005) and defective in aspects of cell cycle checkpoint control (Hirai and Wang, 2002; Hopkins et al., 2004) all along the evolutionary tree. These results suggest that the presence of EgRAD9 in FGL and in PSc of *E. granulosus* is related to the survival of the parasite.

We did not observe statistically significant differences in the level of EgRAD9 expression when comparing FGL, IGL, and PSc samples at the protein level. Interestingly, expression of EgRAD9 protein (normalized to EgEF1) was similar in FGL and in PSc treated and non-treated with H_2O_2. These results coincide with those obtained in other eukaryotes, in which the regulation of RAD9 activity is not related to an increase in the level of expression, but rather in the hyperphosphorylation of the protein when cells are treated with DNA damage agents (St Onge et al., 1999; Volkmer and Karnitz, 1999; Yoshida et al., 2003). Thus, Rad9 is found constitutively phosphorylated in multiple residues in the carboxyl-terminal region of the protein (St Onge et al., 1999, 2001) but it is subjected to additional phosphorylation in response to DNA damage. This hyperphosphorylation is fundamental to the cell cycle arrest function of this protein, as it has been found to be involved in the activation of Chk1 (Roos-Mattjus et al., 2003), as well as in the stability and correct functioning of the 9-1-1 complex (St Onge et al., 2003). Coincidentally, our results show a delay in the electrophoretic mobility of EgRAD9 (from ~49 kDa to ~52 kDa) in PSc treated with 10 mM H_2O_2 for 1 h, suggesting hyperphosphorylation of this protein in response to DNA damage. However, we did not visualize this delay in the electrophoretic mobility of EgRAD9 in PSc treated with 1 mM H_2O_2 for 1 h. One possible explanation for this result could be that treatments with 1 mM H_2O_2 produce oxidative DNA damage only in a few PSc cells (see Fig. 1B), resulting in a low proportion of hyperphosphorylated EgRAD9. Indeed,

experiments performed by Molina-Lopez et al. (2006) indicate that the platyhelminth parasite *Taenia crassiceps* tolerates concentrations of 2.5 mM H_2O_2 during 2.5 h of exposure, preserving motility and parasite morphological traits intact. However, concentrations of 4 mM H_2O_2 turned out to be lethal to the parasite. Moreover, Yoshida et al. (2003) reported that U-937 human cell treatment with the genotoxic agent 1-β-d-arabinofuranosylcytosine (ara-C) in concentrations of 1 μM during 2 h induces a slight delay in electrophoretic mobility of hRad9. However, electrophoretic delay is greater after employing concentrations of 10 μM ara-C during 2 h. Likewise, Chen et al. (2001) indicate that only exposures with 30-Gy of γ rays in YZ5 cells (A-T cells stably transfected with ATM) are capable of inducing hyperphosphorylation of hRad9. 10-Gy exposures do not generate the same effect in the protein. These results strongly suggest that the level of hyperphosphorylation of EgRAD9 correlates with induction of the genotoxic agent in a dose-dependent manner.

In spite of the substantial level of nitric oxide and peroxidation of lipids found in the germinal layer and hydatid fluid of fertile cysts (Amanvermez and Celik, 2002), we only found a slight percentage of DNA damage in FGL nuclei. Consequently, we expected to find hyperphosphorylation of EgRAD9 in this structure of the hydatid cyst, involved in repairing DNA damage produced by ROS and RNS. However, we did not observe hyperphosphorylated EgRAD9 forms in FGL. Together with the effects of dose-dependency of hyperphosphorylation of EgRAD9 to DNA damaging agents previously mentioned, another possible explanation relates to the high levels of antioxidant enzymes in helminths, which in many cases may be found in the host-parasite interphase (Cookson et al., 1992; James, 1994). Some studies show that effective protection of parasites in relation to ROS and RNS produced by the host depends on the level of antioxidant enzymes. Thus, reports in the nematode *Nippostrongylus brasiliensis* demonstrates a correlation between the overexpression of superoxide dismutase (SOD), catalase and glutathione peroxidase (GSH-Px) enzymes and the survival and persistence of parasite in the host. Moreover, an increase in the production of ROS by peritoneal lymphocytes correlates with host protection and the death of this parasite (Smith and Bryant, 1989). In *E. granulosus* it has been described the specific enzyme activity of SOD (Lymbery and Thompson, 1988; Salinas and Cardozo, 2000) and glutathione S-transferase (Morello et al., 1982). The latter has been shown to present a protective role against lipid peroxidation in *Trichinella spiralis* (Rojas et al., 1997). Recently, thioredoxin peroxidase (TPx) activities were found in *E. granulosus*, displaying an important antioxidant function against H_2O_2 (Salinas et al., 1998; Li et al., 2004).

In summary, oxidative damage of DNA is part of an infertility-inducing mechanism in hydatid cysts. EgRAD9 is expressed at the mRNA and protein levels in *E. granulosus*. The protein is phosphorylated to a similar extent as RAD9 in other eukaryotes. Molecules involved in DNA repair in the germinal layer of fertile hydatid cysts and in protoscoleces, such as EgRAD9, may allow preserving the fertility of hydatid cysts in the presence of ROS and RNS.

Literature Cited

Adoutte A, Balavoine G, Lartillot N, Lespinet O, Prud'homme B, de RR. 2000. The new animal phylogeny: Reliability and implications. Proc Natl Acad Sci USA 97:4453–4456.

Amanvermez R, Celik C. 2002. Effectiveness of free radicals in hydatid cysts. J Egypt Soc Parasitol 32:259–269.

Bortoletti G, Ferretti G. 1978. Ultrastructural aspects of fertile and sterile cysts of Echinococcus granulosus developed in hosts of different species. Int J Parasitol 8:421–431.

Bradford MM. 1976. A rapid and sensitive method for the quantitation of microgram quantities of protein utilizing the principle of protein-dye binding. Anal Biochem 72:248–254.

Budke CM. 2006. Global socioeconomic impact of cystic echinococcosis. Emerg Infect Dis 12:296–303.

Callahan HL, Crouch RK, James ER. 1988. Helminth anti-oxidant enzymes: A protective mechanism against host oxidants? Parasitol Today 4:218–225.

Chang DY, Lu AL. 2005. Interaction of checkpoint proteins Hus1/Rad1/Rad9 with DNA base excision repair enzyme MutY homolog in fission yeast, Schizosaccharomyces pombe. J Biol Chem 280:408–417.

Chen MJ, Lin YT, Lieberman HB, Chen G, Lee EY. 2001. ATM-dependent phosphorylation of human Rad9 is required for ionizing radiation-induced checkpoint activation. J Biol Chem 276:16580–16586.

Conchedda M, Gabriele E, Bortoletti G. 2004. Immunobiology of cystic echinococcosis. Parassitologia 46:375–380.

Cookson E, Blaxter ML, Selkirk ME. 1992. Identification of the major soluble cuticular glycoprotein of lymphatic filarial nematode parasites (gp29) as a secretory homolog of glutathione peroxidase. Proc Natl Acad Sci USA 89:5837–5841.

da Silva CM, Ferreira HB, Picon M, Gorfinkiel N, Ehrlich R, Zaha A. 1993. Molecular cloning and characterization of actin genes from Echinococcus granulosus. Mol Biochem Parasitol 60:209–219.

Dang T, Bao S, Wang XF. 2005. Human Rad9 is required for the activation of S-phase checkpoint and the maintenance of chromosomal stability. Genes Cells 10:287–295.

Davey HW, Kelly JK, Wildeman AG. 1995. The nucleotide sequence, structure, and preliminary studies on the transcriptional regulation of the bovine alpha skeletal actin gene. DNA Cell Biol 14:609–618.

Dean FB, Lian L, O'Donnell M. 1998. cDNA cloning and gene mapping of human homologs for Schizosaccharomyces pombe rad17, rad1, and hus1 and cloning of homologs from mouse, Caenorhabditis elegans, and Drosophila melanogaster. Genomics 54:424–436.

Dzik JM. 2006. Molecules released by helminth parasites involved in host colonization. Acta Biochim Pol 53:33–64.

Eckert J, Deplazes P. 2004. Biological, epidemiological, and clinical aspects of echinococcosis, a zoonosis of increasing concern. Clin Microbiol Rev 17:107–135.

Fraga CG, Shigenaga MK, Park JW, Degan P, Ames BN. 1990. Oxidative damage to DNA during aging: 8-hydroxy-2′-deoxyguanosine in rat organ DNA and urine. Proc Natl Acad Sci USA 87:4533–4537.

Furtado C, Regis-da-Silva CG, Passos-Silva DG, Franco GR, Macedo AM, Junho Pena SD, Machado CR. 2007. Schistosoma mansoni: The IMP4 gene is involved in DNA repair/tolerance after treatment with alkylating agent methyl methane sulfonate. Exp Parasitol 116:25–34.

Galindo M, Gonzalez MJ, Galanti N. 2002. Echinococcus granulosus protoscolex formation in natural infections. Biol Res 35:365–371.

Galindo M, Paredes R, Marchant C, Mino V, Galanti N. 2003. Regionalization of DNA and protein synthesis in developing stages of the parasitic platyhelminth Echinococcus granulosus. J Cell Biochem 90:294–303.

Gembka A, Toueille M, Smirnova E, Poltz R, Ferrari E, Villani G, Hubscher U. 2007. The checkpoint clamp, Rad9-Rad1-Hus1 complex, preferentially stimulates the activity of apurinic/apyrimidinic endonuclease 1 and DNA polymerase beta in long patch base excision repair. Nucleic Acids Res 35:2596–2608.

Gutfeld O, Prus D, Ackerman Z, Dishon S, Linke RP, Levin M, Urieli-Shoval S. 2006. Expression of serum amyloid A, in normal, dysplastic, and neoplastic human colonic mucosa: Implication for a role in colonic tumorigenesis. J Histochem Cytochem 54:63–73.

Hang H, Rauth SJ, Hopkins KM, Davey SK, Lieberman HB. 1998. Molecular cloning and tissue-specific expression of Mrad9, a murine orthologue of the Schizosaccharomyces pombe rad9+ checkpoint control gene. J Cell Physiol 177:241–247.

Hang H, Rauth SJ, Hopkins KM, Lieberman HB. 2000. Mutant alleles of Schizosaccharomyces pombe rad9(+) alter hydroxyurea resistance, radioresistance and checkpoint control. Nucleic Acids Res 28:4340–4349.

Harman D. 1992. Role of free radicals in aging and disease. Ann NY Acad Sci 673:126–141.

Hirai I, Wang HG. 2002. A role of the C-terminal region of human Rad9 (hRad9) in nuclear transport of the hRad9 checkpoint complex. J Biol Chem 277:25722–25727.

Hirji N, Lin TJ, Bissonnette E, Belosevic M, Befus AD. 1998. Mechanisms of macrophage stimulation through C D8: Macrophage CD8alpha and CD8beta induce nitric oxide production and associated killing of the parasite Leishmania major. J Immunol 160:6004–6011.

Hoeijmakers JH. 2001. Genome maintenance mechanisms for preventing cancer. Nature 411:366–374.

Hopkins KM, Auerbach W, Wang XY, Hande MP, Hang H, Wolgemuth DJ, Joyner AL, Lieberman HB. 2004. Deletion of mouse rad9 causes abnormal cellular responses to DNA damage, genomic instability, and embryonic lethality. Mol Cell Biol 24:7235–7248.

James ER. 1994. Superoxide dismutase. Parasitol Today 10:481–484.

James SL, Glaven J. 1989. Macrophage cytotoxicity against schistosomula of Schistosoma mansoni involves arginine-dependent production of reactive nitrogen intermediates. J Immunol 143:4208–4212.

Kamenetzky L, Canova SG, Guarnera EA, Rosenzvit MC. 2000. Echinococcus granulosus: DNA extraction from germinal layers allows strain determination in fertile and nonfertile hydatid cysts. Exp Parasitol 95:122–127.

Kaneko YS, Watanabe N, Morisaki H, Akita H, Fujimoto A, Tominaga K, Terasawa M, Tachibana A, Ikeda K, Nakanishi M. 1999. Cell-cycle-dependent and ATM-independent expression of human Chk1 kinase. Oncogene 18:3673–3681.

Kang MH, Park EH, Lim CJ. 2007. Protective role and regulation of Rad9 from the fission yeast Schizosaccharomyces pombe. FEMS Microbiol Lett 275:270–277.

Kobayashi M, Hirano A, Kumano T, Xiang SL, Mihara K, Haseda Y, Matsui O, Shimizu H, Yamamoto K. 2004. Critical role for chicken Rad17 and Rad9 in the cellular response to DNA damage and stalled DNA replication. Genes Cells 9:291–303.

Li J, Zhang WB, Loukas A, Lin RY, Ito A, Zhang LH, Jones M, McManus DP. 2004. Functional expression and characterization of Echinococcus granulosus thioredoxin peroxidase suggests a role in protection against oxidative damage. Gene 326:157–165.

Lieberman HB. 2006. Rad9, an evolutionarily conserved gene with multiple functions for preserving genomic integrity. J Cell Biochem 97:690–697.

Lieberman HB, Hopkins KM, Nass M, Demetrick D, Davey S. 1996. A human homolog of the Schizosaccharomyces pombe rad9+ checkpoint control gene. Proc Natl Acad Sci USA 93:13890–13895.

Liu Q, Guntuku S, Cui XS, Matsuoka S, Cortez D, Tamai K, Luo G, Carattini-Rivera S, DeMayo F, Bradley A, Donehower LA, Elledge SJ. 2000. Chk1 is an essential kinase that is regulated by Atr and required for the G(2)/M DNA damage checkpoint. Genes Dev 14:1448–1459.

Lopez-Moreno HS. 2002. Tissular cestodiasis: Role of helper type 1 and 2 t-lymphocytes. Salud Publica Mex 44:145–152.

Lymbery AJ, Thompson RC. 1988. Electrophoretic analysis of genetic variation in Echinococcus granulosus from domestic hosts in Australia. Int J Parasitol 18:803–811.

Machella N, Regoli F, Santella RM. 2005. Immunofluorescent detection of 8-oxo-dG and PAH bulky adducts in fish liver and mussel digestive gland. Aquat Toxicol 71:335–343.

Martinez C, Paredes R, Stock RP, Saralegui A, Andreu M, Cabezon C, Ehrlich R, Galanti N. 2005. Cellular organization and appearance of differentiated structures in developing stages of the parasitic platyhelminth Echinococcus granulosus. J Cell Biochem 94:327–335.
McManus DP, Zhang W, Li J, Bartley PB. 2003. Echinococcosis. Lancet 362:1295–1304.
Molina-Lopez J, Jimenez L, Ochoa-Sanchez A, Landa A. 2006. Molecular cloning and characterization of a 2-Cys peroxiredoxin from Taenia solium. J Parasitol 92:796–802.
Morello A, Repetto Y, Atias A. 1982. Characterization of glutathione S-transferase activity in Echinococcus granulosus. Comp Biochem Physiol B 72:449–452.
Murray JM, Carr AM, Lehmann AR, Watts FZ. 1991. Cloning and characterisation of the rad9 DNA repair gene from Schizosaccharomyces pombe. Nucleic Acids Res 19:3525–3531.
Paredes R, Jimenez V, Cabrera G, Iraguen D, Galanti N. 2007. Apoptosis as a possible mechanism of infertility in Echinococcus granulosus hydatid cysts. J Cell Biochem 100:1200–1209.
Parrilla-Castellar ER, Arlander SJ, Karnitz L. 2004. Dial 9-1-1for DNA damage: The Rad9-Hus1-Rad1 (9-1-1) clamp complex. DNA Repair (Amst) 3:1009–1014.
Rigano R, Profumo E, Ioppolo S, Notargiacomo S, Ortona E, Teggi A, Siracusano A. 1995. Immunological markers indicating the effectiveness of pharmacological treatment in human hydatid disease. Clin Exp Immunol 102:281–285.
Rigano R, Buttari B, Profumo E, Ortona E, Delunardo F, Margutti P, Mattei V, Teggi A, Sorice M, Siracusano A. 2007. Echinococcus granulosus antigen B impairs human dendritic cell differentiation and polarizes immature dendritic cell maturation towards a Th2 cell response. Infect Immun 75:1667–1678.
Riley PA. 1994. Free radicals in biology: Oxidative stress and the effects of ionizing radiation. Int J Radiat Biol 65:27–33.
Rojas J, Rodriguez-Osorio M, Gomez-Garcia V. 1997. Immunological characteristics and localization of the Trichinella spiralis glutathione S-transferase. J Parasitol 83:630–635.
Roos-Mattjus P, Vroman BT, Burtelow MA, Rauen M, Eapen AK, Karnitz LM. 2002. Genotoxin-induced Rad9-Hus1-Rad1 (9-1-1) chromatin association is an early checkpoint signaling event. J Biol Chem 277:43809–43812.
Roos-Mattjus P, Hopkins KM, Oestreich AJ, Vroman BT, Johnson KL, Naylor S, Lieberman HB, Karnitz LM. 2003. Phosphorylation of human Rad9 is required for genotoxin-activated checkpoint signaling. J Biol Chem 278:24428–24437.
Rucklidge GJ, Milne G, Chaudhry SM, Robins SP. 1996. Preparation of biotinylated, affinity-purified antibodies for enzyme-linked immunoassays using blotting membrane as an antigen support. Anal Biochem 243:158–164.
Salinas G, Cardozo S. 2000. Echinococcus granulosus: Heterogeneity and differential expression of superoxide dismutases. Exp Parasitol 94:56–59.
Salinas G, Fernandez V, Fernandez C, Selkirk ME. 1998. Echinococcus granulosus: Cloning of a thioredoxin peroxidase. Exp Parasitol 90:298–301.
Shepherd JC, Aitken A, McManus DP. 1991. A protein secreted in vivo by Echinococcus granulosus inhibits elastase activity and neutrophil chemotaxis. Mol Biochem Parasitol 44:81–90.
Smith NC, Bryant C. 1989. The effect of antioxidants on the rejection of Nippostrongylus brasiliensis. Parasite Immunol 11:161–167.
St Onge RP, Udell CM, Casselman R, Davey S. 1999. The human G2 checkpoint control protein hRAD9 is a nuclear phosphoprotein that forms complexes with hRAD1 and hHUS1. Mol Biol Cell 10:1985–1995.
St Onge RP, Besley BD, Park M, Casselman R, Davey S. 2001. DNA damage-dependent and -independent phosphorylation of the hRad9 checkpoint protein. J Biol Chem 276:41898–41905.
St Onge RP, Besley BD, Pelley JL, Davey S. 2003. A role for the phosphorylation of hRad9 in checkpoint signaling. J Biol Chem 278:26620–26628.
Steers NJ, Rogan MT, Heath S. 2001. In-vitro susceptibility of hydatid cysts of Echinococcus granulosus to nitric oxide and the effect of the laminated layer on nitric oxide production. Parasite Immunol 23:411–417.
Stergiou L, Hengartner MO. 2004. Death and more: DNA damage response pathways in the nematode C. elegans. Cell Death Differ 11:21–28.
Thelen MP, Venclovas C, Fidelis K. 1999. A sliding clamp model for the Rad1 family of cell cycle checkpoint proteins. Cell 96:769–770.
Touil-Boukoffa C, Bauvois B, Sanceau J, Hamrioui B, Wietzerbin J. 1998. Production of nitric oxide (NO) in human hydatidosis: Relationship between nitrite production and interferon-gamma levels. Biochimie 80:739–744.
Venclovas C, Thelen MP. 2000. Structure-based predictions of Rad1, Rad9, Hus1 and Rad17 participation in sliding clamp and clamp-loading complexes. Nucleic Acids Res 28:2481–2493.
Volkmer E, Karnitz LM. 1999. Human homologs of Schizosaccharomyces pombe rad1, hus1, and rad9 form a DNA damage-responsive protein complex. J Biol Chem 274:567–570.
Vuitton DA. 2003. The ambiguous role of immunity in echinococcosis: Protection of the host or of the parasite? Acta Trop 85:119–132.
Wang D, Kreutzer DA, Essigmann JM. 1998. Mutagenicity and repair of oxidative DNA damage: insights from studies using defined lesions. Mutat Res 400:99–115.
Webster NR, Nunn JF. 1988. Molecular structure of free radicals and their importance in biological reactions. Br J Anaesth 60:98–108.
Werling D, Piercy J, Coffey TJ. 2006. Expression of TOLL-like receptors (TLR) by bovine antigen-presenting cells-potential role in pathogen discrimination? Vet Immunol Immunopathol 112:2–11.
Yoshida K, Wang HG, Miki Y, Kufe D. 2003. Protein kinase Cdelta is responsible for constitutive and DNA damage-induced phosphorylation of Rad9. EMBO J 22:1431–1441.
Zhou BB, Elledge SJ. 2000. The DNA damage response: Putting checkpoints in perspective. Nature 408:433–439.